SCIENCE CHINA
Earth Sciences

• RESEARCH PAPER •

October 2014 Vol.57 No.10: 2417–2427
doi: 10.1007/s11430-014-4875-7

# Design and testing of a global climate prediction system based on a coupled climate model

MA JieHua[1,2] & WANG HuiJun[1,2*]

[1] *Climate Change Research Center, Chinese Academy of Sciences, Beijing 100029, China;*
[2] *Nansen-Zhu International Research Center, Institute of Atmospheric Physics, Chinese Academy of Sciences, Beijing 100029, China*

Received September 3, 2013; accepted November 4, 2013; published online August 6, 2014

A global climate prediction system (PCCSM4) was developed based on the Community Climate System Model, version 4.0, developed by the National Center for Atmospheric Research (NCAR), and an initialization scheme was designed by our group. Thirty-year (1981–2010) one-month-lead retrospective summer climate ensemble predictions were carried out and analyzed. The results showed that PCCSM4 can efficiently capture the main characteristics of JJA mean sea surface temperature (SST), sea level pressure (SLP), and precipitation. The prediction skill for SST is high, especially over the central and eastern Pacific where the influence of El Niño-Southern Oscillation (ENSO) is dominant. Temporal correlation coefficients between the predicted Niño3.4 index and observed Niño3.4 index over the 30 years reach 0.7, exceeding the 99% statistical significance level. The prediction of 500-hPa geopotential height, 850-hPa zonal wind and SLP shows greater skill than for precipitation. Overall, the predictability in PCCSM4 is much higher in the tropics than in global terms, or over East Asia. Furthermore, PCCSM4 can simulate the summer climate in typical ENSO years and the interannual variability of the Asian summer monsoon well. These preliminary results suggest that PCCSM4 can be applied to real-time prediction after further testing and improvement.

**climate model, climate prediction, ENSO, monsoon**

**Citation:** Ma J H, Wang H J. 2014. Design and testing of a global climate prediction system based on a coupled climate model. Science China: Earth Sciences, 57: 2417−2427, doi: 10.1007/s11430-014-4875-7

China is located in the East Asian monsoon region, with large inter-annual climate variability and frequent drought and flood events. Therefore, short-term climate prediction is important for disaster prevention and mitigation. Since the 1980s, thanks to Chinese scientists' unremitting efforts, many achievements have been made in short-term climate prediction in China.

At present, two categories of approach are used in climate prediction: the statistical methods based on statistical analysis and the dynamical methods based on the rules of variation within the climate system. The dynamical methods also encompass methods based on climate models, and because of the use of increasingly sophisticated climate models and high-performance computing, such methods enable us to obtain next-month, next-season, or even longer timescales of prediction of the climate system. Thus far, dynamic prediction has been carried out mainly by tier-two (T2) (Bengtsson et al., 1993) and tier-one (T1) (Kanamitsu et al., 2002; Palmer et al., 2004; Saha et al., 2006) prediction systems. In the T2 system, seasonal prediction is performed using an atmospheric general circulation model (AGCM) only, with prescribed SST boundary conditions, which themselves have been previously predicted by a coupled GCM or statistical model (Lang et al., 2004). However, owing to insufficient feedback from the atmosphere to the oceans, land and sea ice in AGCMs, the T2 system is limited by the AGCM's passive response to the given boundary

*Corresponding author (email: wanghj@mail.iap.ac.cn)

conditions. Given these constraints, T1-type prediction systems based on coupled climate models have emerged as the mainstream approach (Kanamitsu et al., 2002; Palmer et al., 2004; Saha et al., 2006); their ability to represent the physical interactions between each of the sub-systems leads to more realistic results.

Studies into the dynamic prediction of summer precipitation began in 1988 at the Institute of Atmospheric Physics, Chinese Academy of Science (IAP-CAS) (Zeng et al, 1990). Since then, the first and second generations of the IAP seasonal climate prediction systems (IAP DCP-I and IAP DCP-II) (Zeng et al., 1997, 2003), as well as a seasonal prediction system based on IAP9L-AGCM (Lang et al., 2003, 2004), have been established. Taking the aforementioned limitations of T2 systems into consideration, here we aimed to establish a T1-type system based on a coupled climate system model.

## 1 Model description and prediction system design

### 1.1 Model

The model used in the study was the Community Climate System Model, version 4.0 (CCSM4.0), developed by the National Center for Atmospheric Research (NCAR). The CCSM series has been developed and improved from CCSM1.0 (1996), CCSM2.0 (2002), CCSM3.0 (2004), CCSM4.0 (2010), to the Community Earth System Model (CESM). CCSM4.0 is a global ocean-atmosphere-land-sea-ice coupled climate model, and was released in April 2010 with notable enhancements over CCSM3.0 (Gent et al., 2011). CCSM4.0 consists of four geophysical models: the Community Atmosphere Model, version 4 (CAM4); the Sea-ice Model, version 4 (CICE4); the Community Land Model, version 4 (CLM4); and an ocean model. In addition, a coupler coordinates the four geophysical models and passes information between them. The model is open-sourced and supports different resolutions and combinations of the four geophysical models in order to meet different needs of research, such as simulation of past, present, and future climate change.

A medium resolution and finite volume (FV) dynamical core were selected for this study. In fact, the FV dynamical core has now been made the default option (since CCSM4) because of its superior transport properties compared to the spectrum dynamical core. CAM4 has a horizontal resolution of 2.5° (long.)×1.9° (lat.), 26 vertical hybrid levels, and some notable improvements compared with its former version. CLM4 has the same horizontal resolution as CAM4, can contain different land surface types and plant function types in each grid, and features other noticeable improvements as well (Lawrence et al., 2011). The slab ocean model (SOM), which was chosen for this study as the oceanic component of CCSM4.0, has a rotating coordinate with a horizontal resolution of approximately 1°, and can reproduce the climatology of SST and sea-ice in CCSM4. CICE4 has the same land-sea distribution and horizontal resolution as SOM. For more details regarding CICE4, readers are referred to Holland et al. (2012).

### 1.2 Data and initialization

The central issue in establishing a T1 prediction system is the initialization of the coupled climate model. In this study, the initialization scheme is as follows.

(1) CAM4 was initialized with NCEP Reanalysis 1 data (Kalnay et al., 1996) for 1981–1999 and NCEP FNL data from 2000 after interpolation to the horizontal resolution used in CAM4. The multilevel fields (specific humidity, temperature, zonal and meridional winds) were interpolated from pressure levels to the 26 hybrid levels of CAM4. A single-level field used in the initialization was surface pressure.

(2) CLM4 was initialized with daily soil temperature and soil moisture data taken from the NCEP's Climate Forecast System Reanalysis (CFSR; Saha et al., 2010). The vertical structure of CLM4 and the CFSR data are different. The CFSR soil data are reported in four layers, with depths of 0.1, 0.4, 1.0, and 2.0 m, whereas the CLM4 soil column consists of 15 soil layers: 0.007100635, 0.027925, 0.062258574, 0.118865067, 0.212193396, 0.366065797, 0.619758498, 1.03802705, 1.727635309, 2.864607113, 4.739156711, 7.829766507, 12.92532062, 21.32646906, and 35.17762121 m.

In order to import the observed soil anomalies and overcome the mismatch between the reanalysis data and the model climatology, a normalized anomaly coupling scheme was used in the CLM4 initialization. We first computed the anomalies of the initial soil moisture and soil temperature from the long-term daily climatology, normalized them by their standard deviations, and then combined those initial soil anomalies with the means and standard deviations of soil climatology of CLM output data.

The scheme is expressed mathematically as

$$\frac{\mathrm{CFSR}-\overline{\mathrm{CFSR}}}{\sigma_{\mathrm{CFSR}}}\times\sigma_{\mathrm{CLM}}+\overline{\mathrm{CLM}},$$

where CFSR is the initial soil temperature or soil moisture of CFSR, $\overline{\mathrm{CFSR}}$ is the climatology of CFSR, $\sigma_{\mathrm{CFSR}}$ is the standard deviation of CFSR, $\sigma_{\mathrm{CLM}}$ is the standard deviation of CLM4, and $\overline{\mathrm{CLM}}$ is the climatology of CLM4.

The initial soil conditions were created by imposing the initial normalized anomaly for the layer containing the depth of the CLM layer onto the CLM4 climatology. The layers below 2.0 m were set to model climatology.

(3) SOM was initialized with the anomalies of monthly mean 0–155-m weighted-average salinity, temperature, and sea surface current speed of the NCEP's global ocean data

assimilation system (GODAS) dataset. The GODAS meridional domain covers 74.5°S–64.5°N, whereas the SOM domain is global. The GODAS fields were interpolated to the horizontal resolution used in SOM. Climatological data of SOM were used in regions where GODAS data were undefined. SOM needed not only initialization but also the heat flux at the lower boundary of the mixed layer, which was set to the climatological monthly conditions based on a long simulation of CCSM4.0.

(4) The sea-ice initial conditions were set to the climatological daily conditions based on a long simulation of CCSM4. No observational information was included in the sea-ice initial conditions.

(5) Seven members were chosen according to the lagged average forest (LAF; Hoffman and Kalnay, 1983) scheme for the forecast. The corresponding initial conditions of CAM4, CLM4, and CICE4 were chosen from 28/04 to 04/05 at 24-h intervals, with the same ocean initial conditions. We chose May–June–July–August of 1981–2010 as the integration period for the one-month-lead prediction of boreal summer climate. The prediction results were the seven-member ensemble mean and the climatology was the long-term mean over 30 years.

For evaluation of the prediction results we used the Global Precipitation Climatology Project (GPCP), version 2.2, combined precipitation dataset (Alder et al., 2003), which has a 2.5°×2.5° horizontal resolution. Sea surface temperature (SST) data obtained from the Hadley Centre SST dataset (Rayner et al., 2006) were also used. The Niño1+2, Niño3, Niño4, and Niño3.4 SST indices were obtained from the U.S. Climate Prediction Center. Geopotential height, wind, and sea level pressure (SLP) data were obtained from the NCEP Reanalysis 1 dataset (Kalnay et al., 1996).

## 2 PCCSM4 simulation and prediction

We established a global seasonal prediction system (PCCSM4) based on CCSM4.0 and the initialization scheme. It can predict the global oceanic and atmospheric circulation and regional climate in advance. We carried out 30-year retrospective predictions (1981–2010) to evaluate the prediction sill of PCCSM4.

### 2.1 Seasonal mean bias

Figure 1 shows the observed and PCCSM4-simulated JJA mean SST. The PCSSM4 climatology generally matches the observed patterns: SST is higher in low latitudes and lower in high latitudes. The highest SST is located in the warm pool of the equatorial western Pacific and tropical Indian Ocean. In the equatorial eastern Pacific there is a cold tongue region westward along the equator.

PCCSM4 simulated the main precipitation belt in the tropics and arid regions in the sub-tropics reasonably well (Figure 2). However, there is an obvious "double ITCZ" characteristic with excessive precipitation along the South Pacific Convergence Zone (SPCZ) area, and a westward shift of the rainfall center over the North Pacific Convergence Zone (NPCZ). Besides, the precipitation simulated by PCCSM4 over the Arabian Sea and southern and eastern Tibetan Plateau is more than that in GPCP data. Furthermore, a dry bias over the equatorial West Pacific, northern parts of Eurasia, and South America can be seen.

### 2.2 Prediction skill of PCCSM4

The skill in predicting SST is crucial to the T1 prediction system. To examine the seasonal mean SST prediction skill, the correlation coefficients between observed and reforecast anomalies were calculated for the ensemble mean over a 30-year period. Figure 3 shows the JJA mean seasonal SST prediction skill. In most parts of the global ocean, the temporal correlation coefficients (TCCs) are positive, with areas of statistical significance at the 95% level covering most parts of the Pacific and some parts of the Indian Ocean, especially over the tropical Pacific where the influence of El Niño-Southern Oscillation (ENSO) is dominant. However, the TCCs are relatively low over the South Atlantic, south-

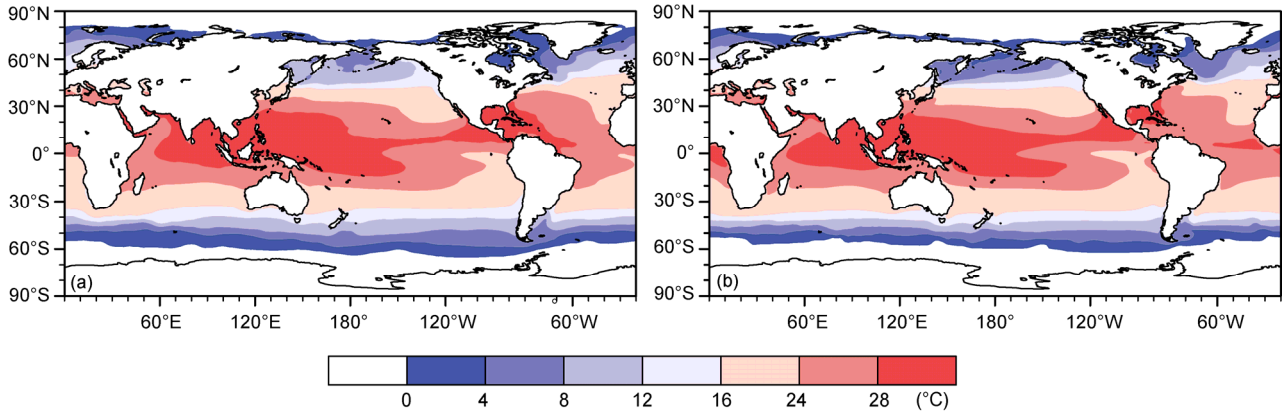


**Figure 1** JJA mean SST (°C) of (a) Hadley SST data and (b) PCCSM4.

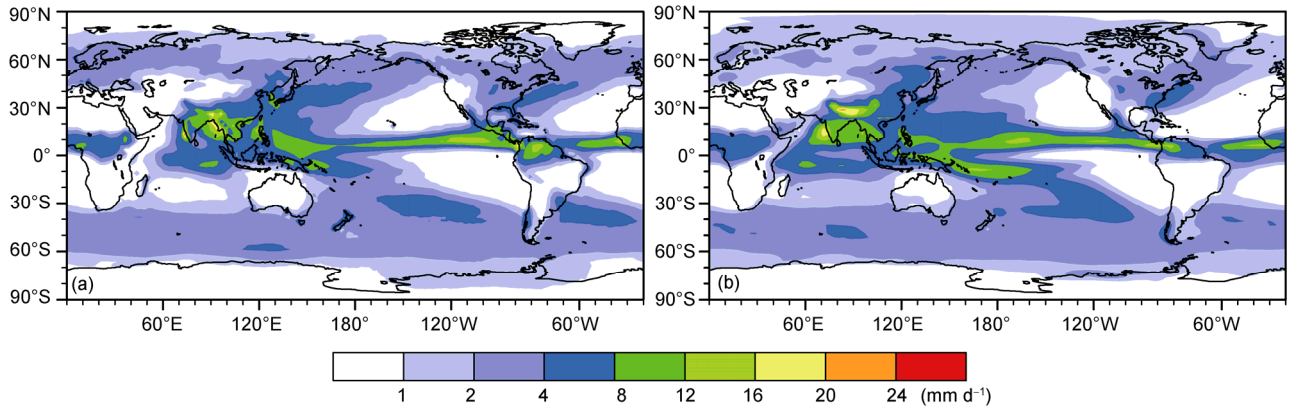


**Figure 2** JJA mean precipitation of (a) GPCP and (b) PCCSM4.

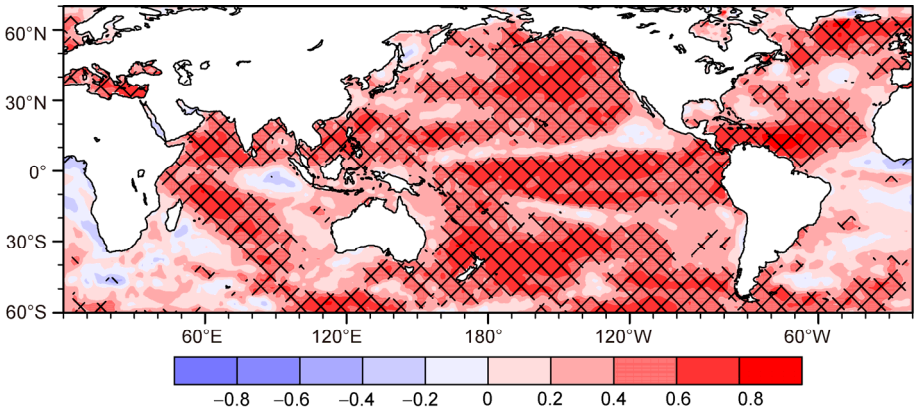


**Figure 3** TCCs for JJA mean SST between PCCSM4 and Hadley data (crossed lines represent areas of statistical significance at the 95% confidence level).

ern parts of the cold tongue region, and several key areas of air-sea interaction, such as the Indonesian Seas and Pacific Ocean, the Kuroshio area and the Gulf Stream area.

As the strongest inter-annual variability phenomenon, ENSO, which occurs in the tropics, can have a global impact. Therefore, whether or not PCCSM4 can predict ENSO reasonably is critical to the performance of the system. Figure 4 shows the normalized anomalies of the key area of ENSO. We can see that PCCSM4 has a high prediction skill over the eastern tropical Pacific. The inter-annual SST variability is simulated well and the correlation coefficients are all above 0.6. The high skill of PCCSM4 in predicting the four indices, which are widely used in ENSO monitoring and prediction, gives us confidence regarding its application in real-time prediction.

Figure 5 shows that the skill in predicting SST is still greater than persistence prediction, and the RMSE is lower than persistence prediction from the second month, even though SOM was coupled in PCCSM4.

### 2.3 PCCSM4 prediction skill for the main atmospheric variables

The skill of PCCSM4 in predicting 500-hPa geopotential height is distributed zonally and decreases with increasing latitude, being higher over the tropics (30°S–30°N) (statistically significant at the 95% confidence level; Figure 6(a)). In a previous study, prediction skill was found to decrease with geopotential height (Lang et al., 2004), but in this study we found that PCCSM4 has relatively high prediction skill at low levels (e.g., 700 hPa) (data not shown). To the south of 30°N in China, the TCCs of 500-hPa geopotential height passed the 95% confidence level in the statistical test, indicating that PCCSM4 possesses relatively good prediction skill over this region.

The TCCs for 850-hPa zonal wind were not as high as those for 500-hPa geopotential height. Parts of the Pacific, northeastern Indian Ocean, and equatorial Atlantic show quite high predictability for zonal wind (Figure 6(b)). Meanwhile, the significant positive correlation regions for SLP are seen mainly in the South Pacific, tropical North Pacific (except the warm pool region), tropical Atlantic, Australia, and most parts of Africa (Figure 6(c)). In general, the level of predictability is greater in the oceans than over inland areas. In addition, possibly due to the distribution of land and the oceans, the predictability is larger in the Southern Hemisphere than in the Northern Hemisphere. The skill of PCCSM4 in predicting precipitation is generally

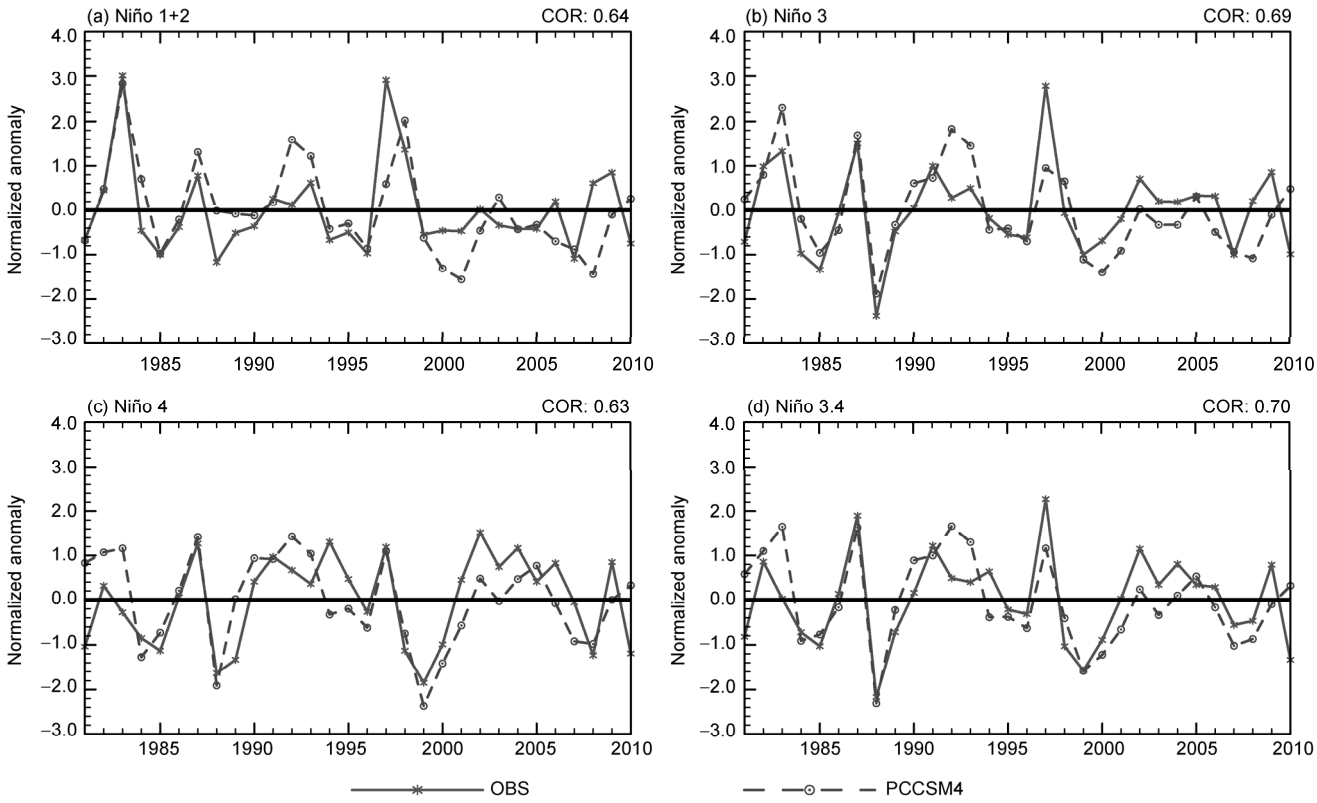


**Figure 4** Normalized anomalies of observed and PCCSM4-predicted Niño 1+2 (0°–10°S, 90°–80°W) (a), Niño 3 (5°N–5°S, 150°–90°W) (b), Niño 4 (5°N–5°S, 160°E–150°W) (c), and Niño3.4 (5°N–5°S, 170°–120°W) (d).

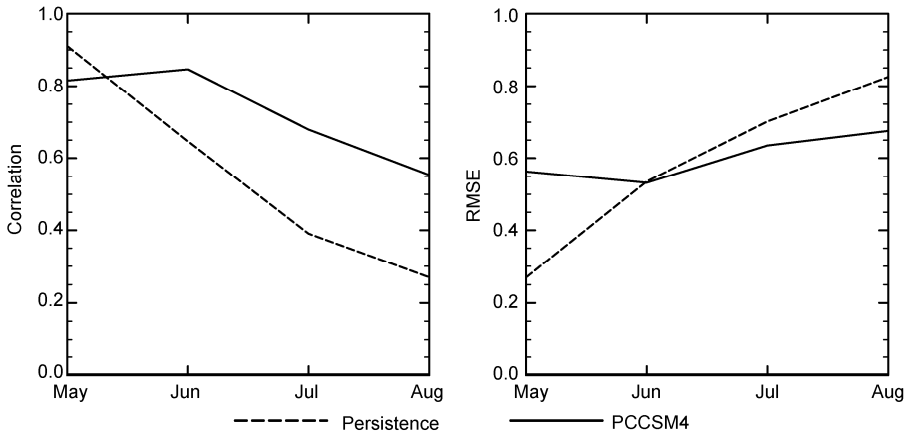


**Figure 5** Prediction skill (a) and RMSE of Niño3.4 SST anomalies (b).

lower than that of circulation variables, with the significant values limited mainly to a narrow belt over the equatorial Pacific and equatorial Atlantic (Figure 6(d)).

As shown in Figure 7(a), the RMSE of 500-hPa geopotential height is mainly below 10 gpm in the tropics and increases with latitude, with the polar regions showing the greatest RMSE. The spatial distribution features were consistent at 300 and 700 hPa (data not shown).

The RMSE of 850-hPa zonal wind is greater in the western equatorial Pacific and eastern equatorial Pacific, which goes against the prediction of ENSO (Figure 7(b)). The greatest RMSE can be found in the mid-latitudes of the Southern Hemisphere, and even the TCCs for 850-hPa zonal wind are higher in this region (Figure 6(b)), the prediction skill over this area is still limited.

The polar regions also show the biggest RMSE of SLP, especially over the Antarctic (Figure 7(c)). The precipitation TCCs in the tropics are high (Figure 6(d)), but the RMSE in this region is high as well (Figure 7(d)). The main center is located in the equatorial Indian Ocean region, east of the

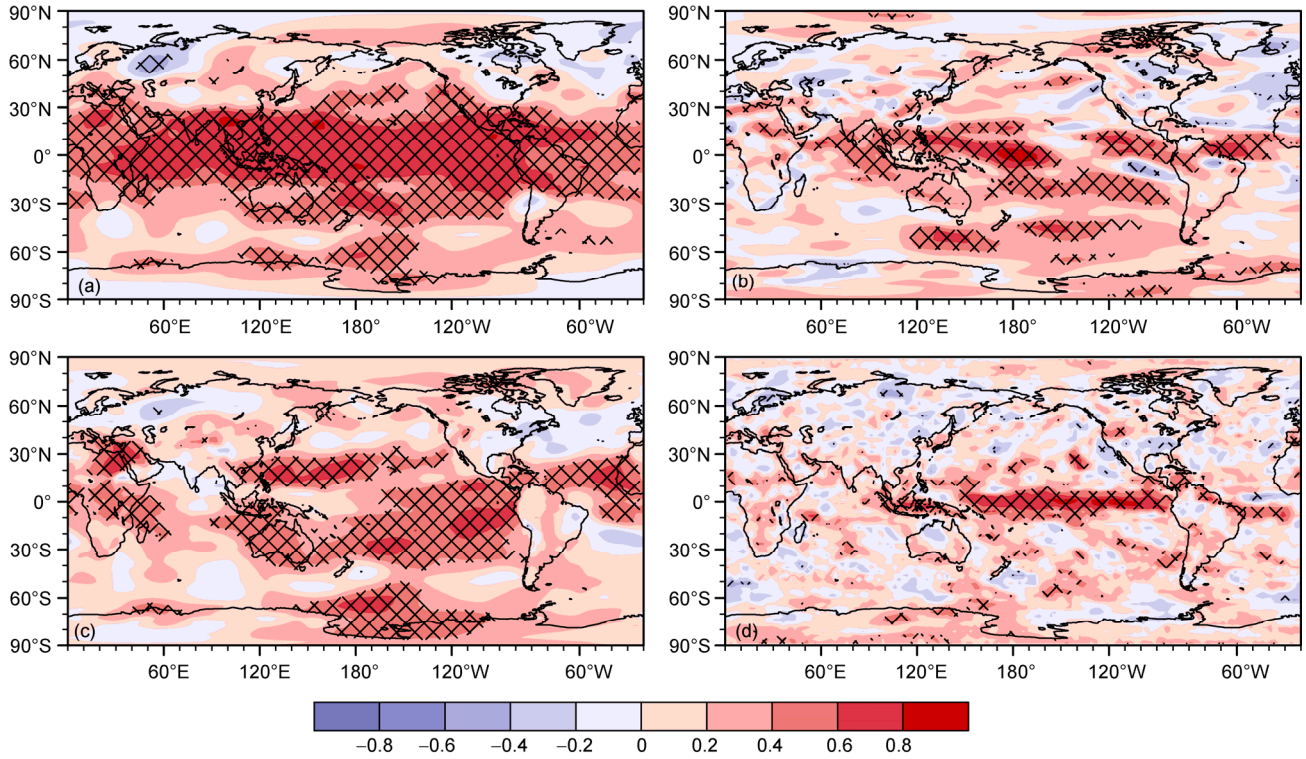


**Figure 6** TCCs of JJA mean 500-hPa geopotential height (a), 850-hPa zonal wind (b), SLP (c), and precipitation (d). Crossed lines indicate statistical significance at the 95% confidence level.

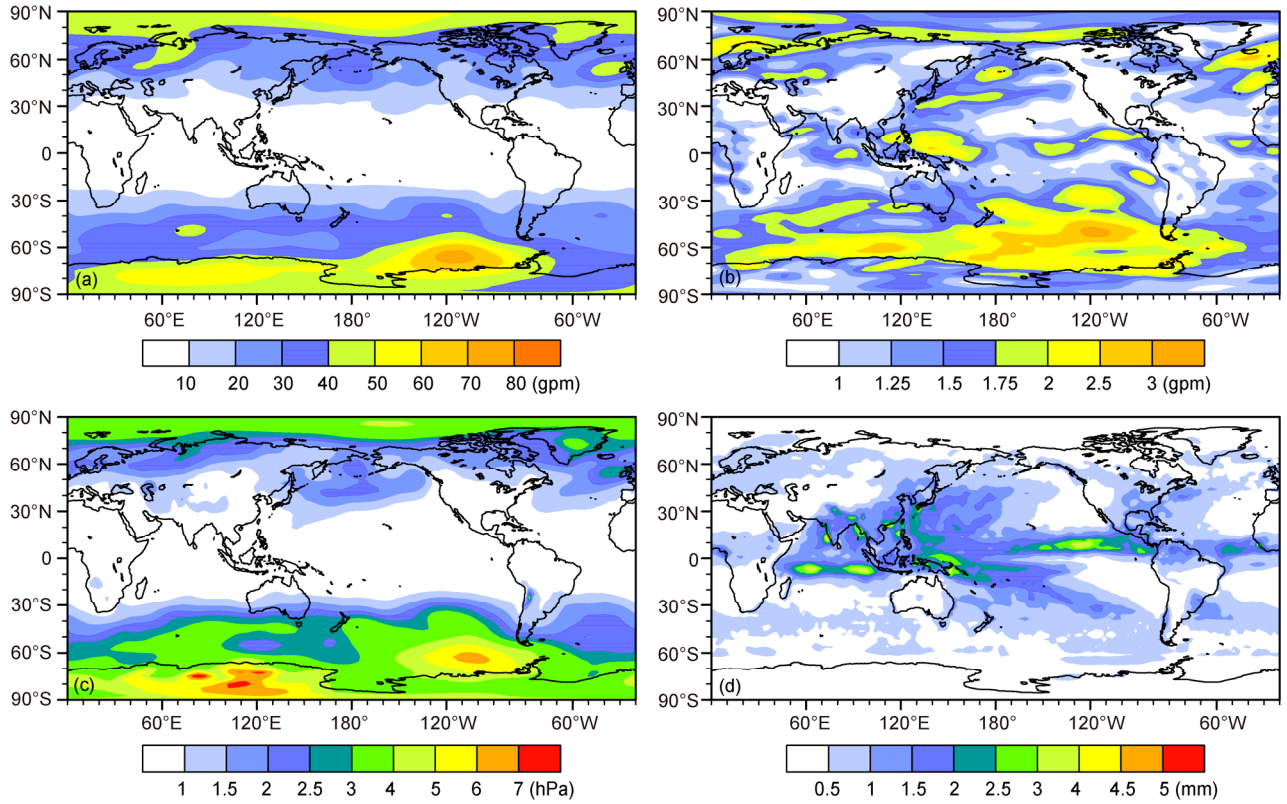


**Figure 7** RMSE of JJA mean 500-hPa geopotential height (gpm) (a), 850-hPa zonal wind (m/s) (b), SLP (hPa) (c), and precipitation (mm/d) (d).

island of New Guinea, and the central and eastern equatorial Pacific. These results indicate difficulties in precipitation simulation and forecasting.

The prediction skill of PCCSM4 is higher in the tropics, with the 30-year mean spatial anomaly correlation coefficients (ACCs) of circulation variables being around 0.3, and that of precipitation up to 0.22, as shown in Table 1. Meanwhile, in East Asia, apart from the 30-year mean SLP spatial ACC, which exceeds 0.2, those of 500-hPa geopotential height, 850-hPa zonal wind, and precipitation are much lower than global (around 0.2) and tropical levels. In general, the predictability of the climate model is higher in the tropics, whereas in the extratropics there is almost no predictability, especially in East Asia. This is a common problem in climate model prediction systems (Wang, 1997).

As shown in Figure 8, there is an obvious inter-annual variability in the spatial ACCs of JJA, with a maximum of 0.5–0.6. The main peaks appear in 1982, 1986, 1987, and 1998, indicating higher prediction skill in extreme climate years. The predictability is greater in the tropics, with positive ACCs in most years and the maximum exceeding 0.6. Meanwhile, the predictability is lower in East Asia, with intense inter-annual variability, the maximum exceeding 0.9, and the minimum approaching -0.9, indicating the complexity and difficulty of climate prediction in this region.

### 2.4 PCCSM4 prediction skill in typical ENSO years

Previous studies have shown that El Niño and La Niña events have a great influence on global climate. As reported above, results showed that PCCSM4 has greater prediction skill in abnormal-climate years. To assess the prediction skill of PCCSM4 for typical ENSO years, we compare the special ACCs in four strong El Niño (1982, 1987, 1997, and 2002) and La Niña (1984, 1988, 1998, and 1999) summers, and normal years (1983, 1995, 1996, and 2001), according to the normalized Niño 3.4 index and Kim et al. (2012). As Table 2 shows, the skill score in strong ENSO years is higher than that in normal years, especially for 500-hPa geopotential height and SLP, with no skill in normal years. The connection between precipitation and ENSO amplitude is the highest, as the correlation coefficients show (statistically significant at the 99% confidence level). The correlation between spatial ACCs of 850-hPa zonal wind and

**Table 1** 30-year mean spatial ACCs for JJA

| | H500 | U850 | SLP | Precipitation |
|---|---|---|---|---|
| Global | 0.18 | 0.22 | 0.18 | 0.20 |
| Tropics | 0.29 | 0.30 | 0.33 | 0.22 |
| East Asia | 0.08 | 0.06 | 0.21 | 0.01 |

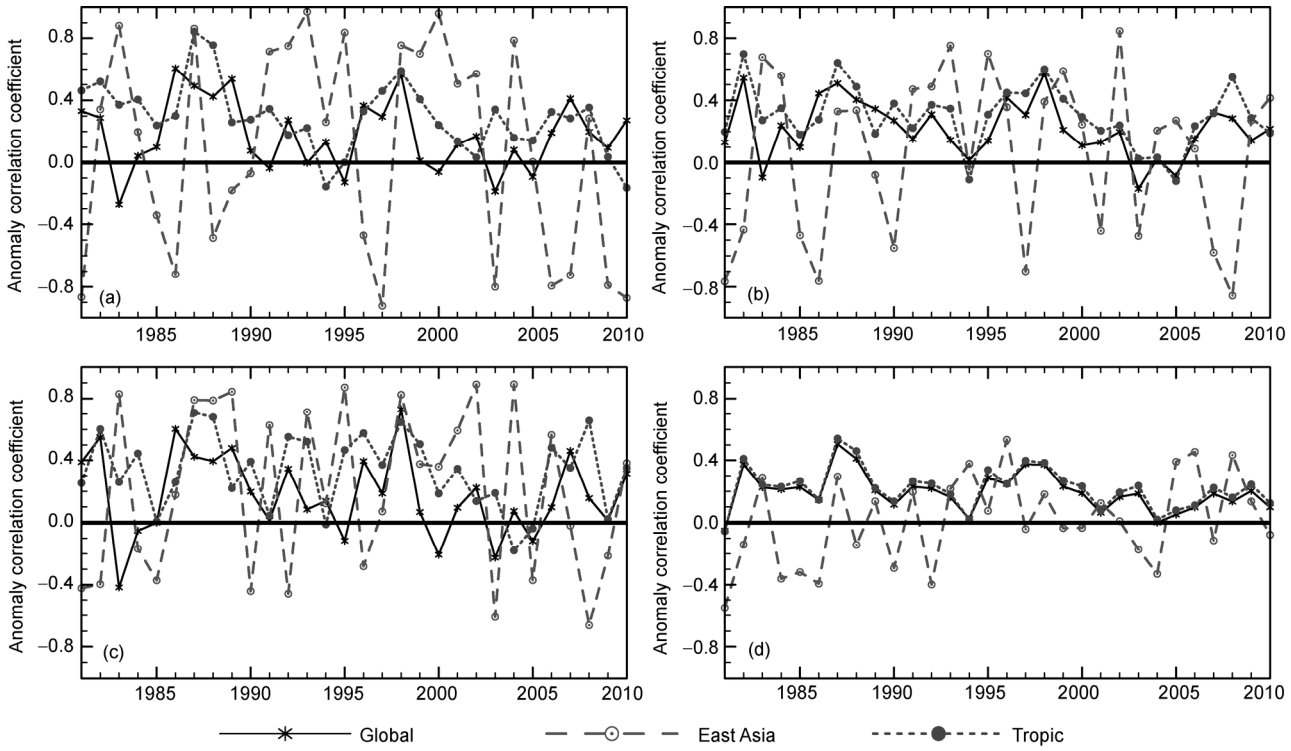


**Figure 8** Spatial ACCs of 500-hPa geopotential height (a), 850-hPa zonal wind (b), SLP (c), and precipitation (d).

**Table 2** Spatial ACCs in different types of years and their correlation with Niño 3.4 index[a)]

| | | H500 | U850 | SLP | Precipitation |
|---|---|---|---|---|---|
| Global | El Niño years | 0.31 | 0.39 | 0.35 | 0.35 |
| | La Niña year | 0.26 | 0.36 | 0.29 | 0.31 |
| | Normal year | 0.02 | 0.15 | –0.01 | 0.21 |
| | Correlation coefficient | 0.32 | 0.35* | 0.25 | 0.55** |
| Tropics | El Niño years | 0.46 | 0.51 | 0.45 | 0.39 |
| | La Niña years | 0.54 | 0.46 | 0.57 | 0.34 |
| | Normal years | 0.21 | 0.31 | 0.41 | 0.23 |
| | Correlation coefficient | 0.43* | 0.34 | 0.17 | 0.56** |
| East Asia | El Niño years | 0.21 | 0.01 | 0.34 | 0.03 |
| | La Niña years | 0.29 | 0.47 | 0.46 | –0.09 |
| | Normal years | 0.13 | –0.20 | 0.09 | –0.01 |
| | Correlation coefficient | –0.08 | 0.11 | 0.23 | –0.12 |

a) * Significant at the 95% confidence level; ** significant at the 99% confidence level.

ENSO amplitude is the second highest, and statistically significant at the 95% confidence level. The results indicate that the skill of PCCSM4 in predicting global precipitation and circulation variables is closely related to ENSO events.

Given that ENSO events occur in the tropical Pacific, they should have the most significant impact in the tropics. Although the predictability is quite high in the tropics, the prediction skill in typical ENSO years is still higher than that in normal years over this region. The correlation coefficient between spatial ACCs of 500-hPa geopotential height (precipitation) and ENSO amplitude is statistically significant at the 95% (99%) confidence level, indicating that ENSO events can affect the geopotential height and precipitation predictability in the tropics.

The relationship between the level of predictability and ENSO events in East Asia is not as close as in global terms or in the tropics, as the results in Table 2 show. However, the prediction skill for 500-hPa geopotential height, 850-hPa zonal wind, and precipitation, in El Niño years is greater than that in normal years. Meanwhile, in La Niña years the prediction skill for 500-hPa geopotential height, 850-hPa zonal wind, and SLP is greater than that in normal years. The prediction skill for East Asian summer precipitation is low in all years, i.e., not only typical ENSO years, but also normal years, indicating that the prediction skill for East Asian summer precipitation is not strongly affected by ENSO. There may be two reasons for this: (1) the relationship between ENSO and East Asian summer precipitation has inter-decadal variations and is not closely related after the 1980s (Wang, 2001, 2002; Gao et al., 2007); and (2) not only the circulation systems in low latitudes, but also those in high latitudes (Zhang et al., 1998; Sun et al., 2012b; Gong et al., 2002), even in the Southern Hemisphere (Wang et al., 2003; Xue et al., 2003; Fan et al., 2004; Wang et al., 2005; Sun et al., 2009; Gao et al., 2003), can impact East Asian summer precipitation and possess complex mechanisms.

### 2.5 Simulation of Asian monsoon indices in PCCSM4

To examine the capability of PCCSM4 in simulating the year-to-year variability of Asian summer monsoon, five commonly used Asian monsoon indices were calculated over 30 years and comparisons made between the hindcasts and reanalyses, as shown in Figure 9. Compared with NCEP reanalysis data, the prediction skill for the interannual variability of Webster-Yang monsoon index (Webster and Yang, 1992) is the worst, with a correlation coefficient of 0.35 (exceeding the 95% significance level; Figure 9a). The correlation coefficients of the other four monsoon indices all exceed 0.5 (statistically significant at the 99% confidence level), meaning PCCSM4 has the ability to capture the interannual variability of the main circulation state over the Asian monsoon region. The high skill in simulating the two East Asian summer monsoon indices (Figure 9(d), (e)) is very encouraging, indicating that even though the prediction skill is very low for East Asian summer precipitation, PCCSM4 can still simulate well the year-to-year variability of East Asian summer monsoon.

## 3 Summary and discussion

PCCSM4 is a global climate prediction system based on CCSM 4.0 and an initialization scheme designed by our group. Its seasonal prediction skill was assessed in the present study through 30-year (1981–2010) retrospective summer climate ensemble predictions.

Despite some model bias, PCCSM4 can efficiently capture the main characteristics of summer climatology. Further analysis showed that the prediction skill for SST is still greater than persistence, even though the oceanic component (SOM) is coupled. The greater predictability of SST in the model covers the main regions of the global ocean; especially over the central and eastern Pacific where the in-

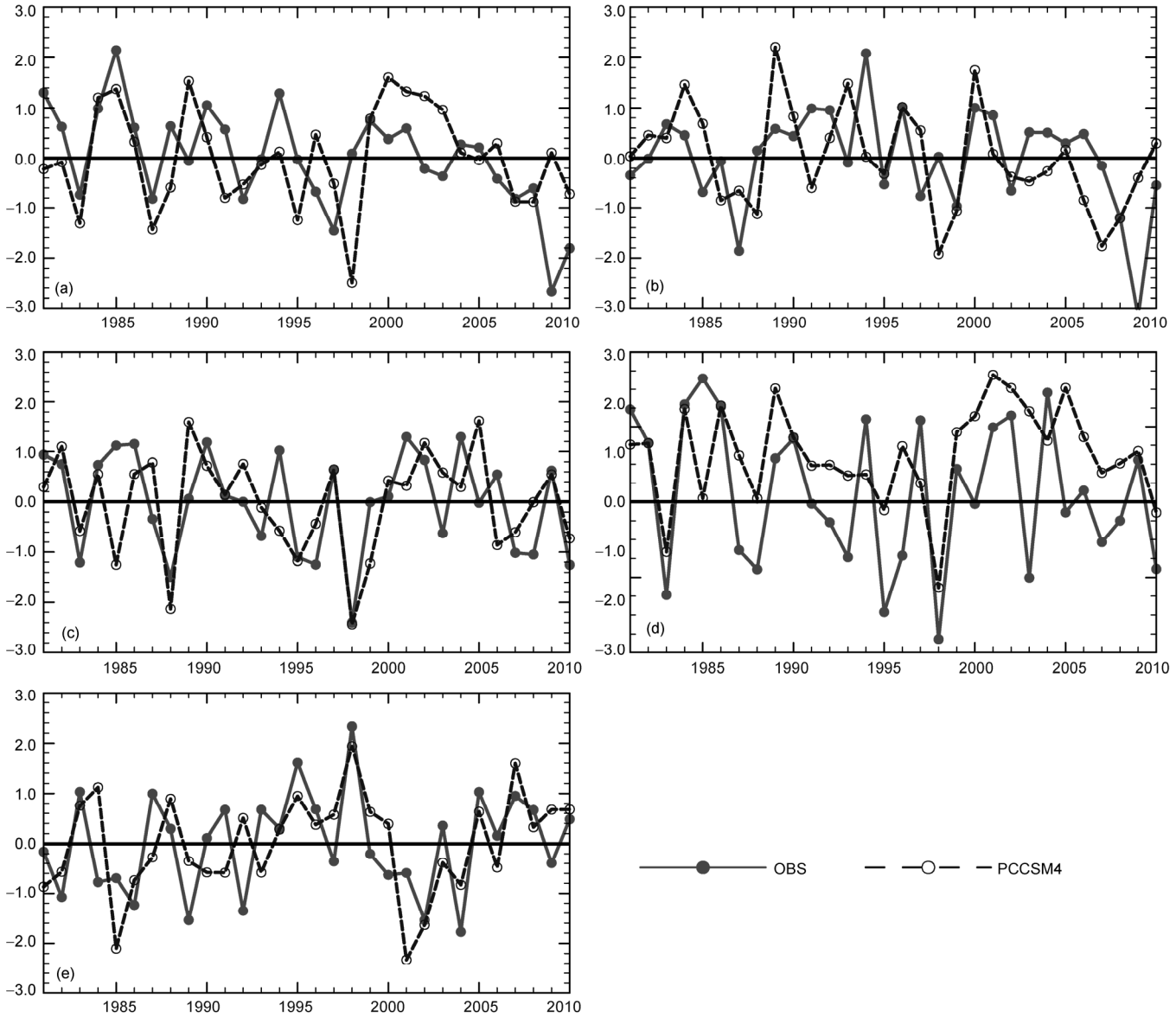


**Figure 9** Asian monsoon indices from 1981 to 2010. (a) Webster-Yang monsoon index (Webster et al., 1992); (b) Indian Monsoon index (Wang et al., 1999); (c) western North Pacific monsoon index (Wang et al., 2001); (d) East Asian summer monsoon index (Zhang et al., 2003); (e) East Asian summer monsoon index (Wang, 2002).

fluence of ENSO is dominant, the SST interannual variability is simulated well. The prediction skill for precipitation is lowest compared with the other variables that were assessed, which is a common limitation of dynamical prediction systems. The prediction skill for 500-hPa geopotential height is highest, and is distributed zonally; the prediction of 850-hPa zonal wind and SLP shows the greatest skill in the tropical oceans, especially in the South Pacific; and high prediction skill for precipitation is limited mainly to a narrow belt over the equatorial Pacific and equatorial Atlantic. In addition, the prediction skill in PCCSM4 shows significant interannual variability, with greater skill in extreme climate years, as demonstrated by the spatial ACC time series results. Furthermore, PCCSM4 shows good capability in simulating the year-to-year variability of the Asian summer monsoon.

Although PCCSM4 can capture the global and tropical summer climate variability well in typical ENSO years and has a high prediction skill for SST anomalies over key ENSO areas, it performs poorly in simulating East Asian summer climate due to the influence of many systems in that region adding an extra degree of complexity. Huang et al. (1989) found that the East Asian summer climate can be affected by ENSO, and later pointed out that SST in the tropical western Pacific warm pool and convective activity can also have an influence (Huang et al., 1993). The complexity of East Asian monsoon variability arises not only from the effects of tropical forcing, but also because of the circulation in high latitudes in the Northern Hemisphere

(Zhang et al., 1998), the West Pacific Subtropical High (Huang et al., 2004), snow cover over the Eurasian continent (Zhao, 1984), Arctic sea ice (Liu et al., 2012), the North Atlantic Oscillation (Gong et al., 2002; Sun et al., 2012b), the Somali Jet (Wang et al., 2003), the Mascarene High and Australian High (Xue et al., 2003), and the Antarctic Oscillation (Gao et al., 2003; Sun et al., 2009), among other factors. Furthermore, due to the interactions between these systems and inter-decadal variability in each system, the variation of East Asian summer climate is complex and difficult to predict.

The prediction skill of dynamical methods over East Asia is severely limited (Wang, 1997), and this was also found for PCCSM4. Although interactions are involved in the T1 method, which is more realistic compared to the T2 method, climate drift is a major challenge in the T1 system. With the limitation of suitable initial observation data, it is hard for the prediction skill in dynamic methods to improve significantly in the short term. Traditionally, statistical error correction methods have been applied to resolving the problem (Zeng et al., 1994; Wang et al., 2000), and in recent years, statistical downscaling methods (Liu et al., 2012a, 2012b; Sun et al., 2012a) and statistical-dynamic hybrid methods have shown promise in short-term climate prediction (Wang et al., 2009; Lang et al., 2010). Therefore, we can explore these methods in the context of PCCSM4 in order to improve its performance over East Asia.

PCCSM4 has greater (less) skill in the tropical belt (mid-high latitudes) due to the stronger internal chaos effect of the atmosphere in mid-high latitudes. Furthermore, the snow cover and sea-ice variations, which have great impacts on climate over the mid-high latitudes, are not involved in PCCSM4. How to improve the initial scheme to involve more observation data is an important issue for improving the prediction skill of PCCSM4 in the future.

*We thank the two anonymous reviewers for their suggestions, which helped to improve the paper. This work was supported by National Natural Science Foundation of China (Grant No. 41130103) and Special Fund for Public Welfare Industry (Meteorology) (Grant No. GYHY201306026).*

Adler R F, Huffman G J, Chang A, et al. 2003. The version-2 global precipitation climatology project (GPCP) monthly precipitation analysis (1979–present). J Hydrometeorol, 4: 1147–1167

Bengtsson L, Schlese U, Roeckner E, et al. 1993. A two-tiered approach to long-range climate forecasting. Science, 261: 1026–1029

Fan K, Wang H J. 2004. Antarctic oscillation and the dust weather frequency in North China, Geophys Res Lett, 31: L10201

Gao H, Wang Y G. 2007. On the weakening relationship between summer precipitation in China and ENSO (in Chinese). Acta Meteorol Sin, 65: 131–137

Gao H, Xue F and Wang H J. 2003. Influence of interannual variability of Antarctic oscillation on mei-yu along the Yangtze and Huaihe River valley and its importance to prediction (in Chinese). Chin Sci Bull, 48: 87–92

Gent P R, Danabasoglu G, Donner L J, et al. 2011. The community climate system model version 4. J Clim, 24: 4973–4991

Gong D Y, Zhu J H and Wang S W. 2002. Significant relationship between spring AO and the summer rainfall along the Yangtze River. Chin Sci Bull, 47: 948–952

Hoffman R N, Kalnay E. 1983. Lagged average forecasting, an alternative to Monte Carlo forecasting. Tellus, 35A: 100–118

Holland M M, Bailey D A, Briegleb B P, et al. 2012. Improved sea ice shortwave radiation physics in CCSM4: The impact of melt ponds and aerosols on Arctic sea ice. J Clim, 25: 1413–1430

Huang J Y, Liu G, Zhao X Y. 2004. The influence of Subtropical High indexes and Polar Vortex indexes on the summertime precipitation in China (in Chinese). Chin J Atoms Sci, 28: 517–526

Huang R H, Sun F Y. 1993. Impacts of the thermal state and the convective activities in the tropical western warm pool on the summer climate anomalies in East Asia (in Chinese). Chin J Atoms Sci, 18: 141–151

Huang R H, Wu Y F. 1989. The influence of ENSO on the summer climate change in China and its mechanism. Adv Atmos Sci, 6: 21–32

Kalnay E, Kanamitsu M, Kistler R, et al. 1996. The NCEP/NCAR 40-year reanalysis project. Bull Amer Meteorol Soc, 77: 437–471

Kanamitsu M, Kumar A, Juang H M H, et al. 2002. NCEP dynamical seasonal forecast system 2000. Bull Amer Meteorol Soc, 83: 1019– 1038

Kim H M, Webster P J, Curry J A, et al. 2012. Asian summer monsoon prediction in ECMWF System 4 and NCEP CFSv2 retrospective seasonal forecasts. Clim Dyn, 39: 2975–2991

Lang X M, Wang H J. 2010. Improving extraseasonal summer rainfall prediction by merging information from GCMs and observations. Weather Forecast, 25: 1263–1274

Lang X M, Wang H J, Zhou G Q. 2003. Real-time prediction of the climate feature for 2003 winter and dust climate for 2004 spring over China (in Chinese). Clim Environ Res, 8: 381–386

Lang X M, Wang H J, Jiang D B. 2004. Extraseasonal short-term predictions of summer climate with IAP9L-AGCM (in Chinese). Chin J Geophys, 47: 19–24

Lawrence D M, Oleson K W, Flanner M G, et al. 2011. Parameterization improvements and functional and structural advances in version 4 of the Community Land Model. J Adv Model Earth Syst, 3: 1–26

Liu J P, Judith A C, Wang H J, et al. 2012. Impact of declining Arctic sea ice on winter snowfall, Proc Natl Acad Sci USA, doi: 10.1073/pnas.1114910109

Liu Y, Fan K. 2012a. Improve the prediction of summer precipitation in the Southeastern China by a hybrid statistical downscaling model. Meteorol Atmos Phys, 117: 121–134

Liu Y, Fan K. 2012b. A new statistical downscaling model for autumn precipitation in China. Inter J Clim, 33: 1321–1336

Palmer T, Andersen U, Cantelaube P, et al. 2004. Development of a European multi-model ensemble system for seasonal to inter-annual prediction (DEMETER). Bull Amer Meteorol Soc, 85: 853–872

Rayner N, Brohan P, Parker D, et al. 2006. Improved analyses of changes and uncertainties in sea surface temperature measured *in situ* since the mid-nineteenth century: The HadSST2 dataset. J Clim, 19: 446–469

Saha S, Nadiga S, Thiaw C, et al. 2006. The NCEP climate forecast system. J Clim, 19: 3483–3517

Saha S, Moorthi S, Pan H-L, et al. 2010. The NCEP climate forecast system reanalysis. Bull Amer Meteorol Soc, 91: 1015–1057

Sun J Q, Chen H P. 2012a. A statistical downscaling scheme to improve global precipitation forecasting. Meteorol Atmos Phys, 117: 87–102

Sun J Q, Wang H J. 2012b. Changes of the connection between the summer North Atlantic Oscillation and the East Asian summer rainfall. J Geophys Res, 117, D08110

Sun J Q, Wang H J, Yuan W. 2009. A possible mechanism for the co-variability of the boreal spring Antarctic Oscillation and the Yangtze River valley summer rainfall. Intl J Clim, 29: 1276–1284

Wang B, Fan Z. 1999. Choice of South Asian summer monsoon indices. Bull Amer Meteorol Soc, 80: 629–638

Wang B, Wu R G, Lau K-M. 2001. Interannual variability of Asian summer monsoon: Contrast between the Indian and western North Pacific-East Asian monsoons. J Clim, 14: 4073–4090

Wang H J. 1997. A preliminary study on the uncertainty of short- term

climate prediction (in Chinese). Clim Environ Res, 2: 333–338
Wang H J. 2001. The weakening of the Asian Monsoon Circulation after the end of 1970's. Adv Atmos Sci, 18, 376–386
Wang H J. 2002. The instability of the East Asian summer monsoon-ENSO relations. Adv Atmos Sci, 19: 1–11
Wang H, Fan K. 2005. Central-north China precipitation as reconstructed from the Qing Dynasty: Signal of the Antarctic Atmospheric Oscillation. Geophys Res Lett, 32, L24705
Wang H J, Fan K. 2009. A new scheme for improving the seasonal prediction of summer precipitation anomalies. Weather Forecast, 24: 548–554
Wang H J, Xue F. 2003. Interannual variability of Somali Jet and its influences on the inter-hemispheric water vapor transport and on the East Asian summer rainfall (in Chinese). Chin J Geophys, 46: 18–25
Wang H J, Zhou G Q and Zhao Y. 2000. An effective method for correcting the seasonal-interannual prediction of summer climate anomaly. Adv Atmos Sci, 17: 234–240
Webster P J, Yang S. 1992. Monsoon and ENSO: Selectively interactive systems. Q J R Meteorol Soc, 118: 877–926
Xue F, Wang H J, He J H. 2003. Interannual variability of Mascarene high and Australian high and their influences on summer rainfall over East Asia. Chin Sci Bull, 48: 492–497
Zeng Q C, Yuan C G, Wang W Q, et al. 1990. Numerical experiment of extraseasonal climate prediction (in Chinese). Chin J Atmos Sci, 14: 10–25
Zeng Q C, Zhang B L, Yuan C G, et al. 1994. A note on some methods suitable for verifying and correcting the prediction of climatic anomaly. Adv Atmos Sci, 11: 121–127
Zeng Q C, Yuan C G, Li X, et al. 1997. Seasonal and extraseasonal predictions of summer monsoon precipitation by gems (1). Adv Atmos Sci, 14: 163–176
Zeng Q C, Lin Z H, Zhou G Q. 2003. Dynamical extraseasonal climate prediction system IAP DCP-II (in Chinese). Chin J Atmos Sci, 27: 289–303
Zhang Q Y, Tao S Y. 1998. Influence of Asian mid-high latitude circulation on East Asian summer rainfall (in Chinese). Acta Meteorol Sin, 56: 199–211
Zhang Q Y, Tao S Y, Chen T L. 2003. The inter-annual variability of East Asian summer monsoon indices and its association with the pattern of general circulation over East Asia (in Chinese). Acta Meteorol Sin, 61: 559–568
Zhao Q. 1984. The snow cover over Eurasia and East Asian summer monsoon (in Chinese). Meteorology, 7: 27–29